



Refined Instrumental Variable method for non-linear dynamic identification of robots

Alexandre Janot, Pierre-Olivier Vandanjon, Maxime Gautier

► To cite this version:

Alexandre Janot, Pierre-Olivier Vandanjon, Maxime Gautier. Refined Instrumental Variable method for non-linear dynamic identification of robots. 2010. <hal-00520261>

HAL Id: hal-00520261

<https://hal.archives-ouvertes.fr/hal-00520261>

Submitted on 22 Sep 2010

HAL is a multi-disciplinary open access archive for the deposit and dissemination of scientific research documents, whether they are published or not. The documents may come from teaching and research institutions in France or abroad, or from public or private research centers.

L'archive ouverte pluridisciplinaire **HAL**, est destinée au dépôt et à la diffusion de documents scientifiques de niveau recherche, publiés ou non, émanant des établissements d'enseignement et de recherche français ou étrangers, des laboratoires publics ou privés.

Refined Instrumental Variable method for non-linear dynamic identification of robots

A. Janot^a, P-O Vandanjon^b, M Gautier^c

^a Haption SA, Laval, France, alexande.janot@haption.com

^b Laboratoire Central des Ponts et Chaussées, Nantes, France, pierre-olivier.vandanjon@lcpc.fr

^c Institut de Recherche en Communication et Cybernétique de Nantes, France, maxime.gautier@ircyn.ec-nantes.fr

Abstract

The identification of the dynamic parameters of robot is based on the use of the inverse dynamic identification model which is linear with respect to the parameters. This model is sampled while the robot is tracking “exciting” trajectories, in order to get an over determined linear system. The linear least squares solution of this system calculates the estimated parameters. The efficiency of this method has been proved through the experimental identification of a lot of prototypes and industrial robots. However, this method needs joint torque and position measurements and the estimation of the joint velocities and accelerations through the bandpass filtering of the joint position at high sample rate. So, the observation matrix is noisy. Moreover identification process takes place when the robot is controlled by feedback. These violations of assumption imply that the LS estimator is not consistent. This paper focuses on the Refined Instrumental Variable (RIV) approach to overcome this problem of noisy observation matrix. This technique is applied to a 2 degrees of freedom (DOF) prototype developed by the IRCCyN Robotic team.

Key words: Identification algorithms, Least-squares methods, Robot dynamics

1. Introduction

The usual identification method based on the inverse dynamic model (IDM) and LS technique has been successfully applied to identify inertial and friction parameters of a lot of prototypes, industrial robots and has been extended to cars, worksite engine, human being and haptic interfaces (Atkeson, An, et Hollerbach 1986)(Swevers et al. 1997)(Khosla et Kanade 1985)(Kozłowski 1998)(Raucent et al. 1992)(Gautier 1986)(Restrepo et Gautier 1995)(Gautier 1997)(Venture et al. 2006) (C-E Lemaire et al. 2006)(Janot et al. 2007) among others. At any case, a derivative bandpass data filtering is required to calculate the joint velocities and accelerations. Moreover identification process is carried out with a feedback controlled robot. These conditions may lead to a violation of statistical independence between the residual and the observation matrix which implies that the LS solution is not consistent. To overcome this problem of noisy observation matrix, several methods have been proposed in the past: Extended Kalman Filtering, total least-squares, Instrumental Variable method .

We show in (Gautier et Poignet 2001) that Extended Kalman Filtering is more complicated without improvements of results.

As far as total least squares are concerned, we used them in order to identify simultaneously dynamic and drive gain parameters (Gautier, P.O. Vandanjon, et Presse 1994). However, we did not succeed in applying this method to take into account the feedback which correlates the noise.

Instrumental Variable method was already applied in robotics (Puthenpura et Sinha 1986). This method was used in order to identify a SISO system linear with respect to the state in an open loop configuration for each axis of an industrial robot. In this paper, the IV is applied for a dynamic model of a robot non linear with respect to the state and in closed loop configuration.

Recently, the Instrumental Variable (IV) approach was renewed in the context of closed loop linear continuous system.

This method is particularly interesting because of its simplicity. Indeed, no noise model identification is needed and the IV estimator is consistent even if the noise is colored (Young et Jakeman 1979), (Söderström et Stoica 1989). However, this technique was generally applied to discrete system linear with respect to the state which is not the case in robotics. The choice of the instrument variable depends on the context. Moreover, the method was designed in open loop system. Progressively, algorithms suitable to our context, i.e. continuous time and closed loop system, have emerged. In particular, the so-called SRIVC

algorithm (Simplified Refined Instrumental Variable Continuous-time) for open loop system, based on an auxiliary model as instrument variable, is a good candidate to our problem (Young 2006). Very recently, this last algorithm was modified in order to take into account closed loop system (Gilson et al. 2006)(Young, Garnier, et Gilson 2009) but still in the frame of system linear with respect to the state. This technique is implemented in the MATLAB CONTSID toolbox developed by the CRAN team (Garnier, Gilson, et Cervellin 2006).

A derivation of this IV method was first successfully applied on a 1 DOF haptic device (P-O. Vandanjon et al. 2007). This derivation is based on the use of both the inverse dynamic model (IDM) and the direct dynamic model (DDM). The robustness to data filtering and to the initialization as the calculation of the optimal solution were presented in (Janot, P-O. Vandanjon, et Gautier 2009). However, the consistence of the estimation (like statistical rules), the convergence of the purposed algorithm and the robustness to control laws were not introduced. This paper deals with these issues and the IV method is carried out on a 2 DOF prototype robot developed by the IRCCyN robotic team. This direct drive prototype is very well suited to our purpose because it emphasizes non linear coupling contrary to industrial robots with high gear ratio.

The paper is organized as follows: section 2 reviews the usual identification technique of the dynamic parameters of the robot. Section 3 presents the Instrumental Variable techniques. The experimental results are given in section 4. Finally, section 5 is the conclusion

2. IDIM

The inverse dynamic model (IDM) of a rigid robot composed of n moving links calculates the motor torque vector τ_{idm} , as a function of the generalized coordinates and their derivatives. It can be obtained from the Newton-Euler or the Lagrangian equations, (W. Khalil et Dombre 2002), (Featherstone et Orin 2008). It is given by the following relation:

$$\tau_{idm} = M(q) \ddot{q} + N(q, \dot{q}) \quad (1)$$

Where, q , \dot{q} and \ddot{q} are respectively the $(nx1)$ vectors of generalized joint positions, velocities and accelerations, $M(q)$ is the $(n \times n)$ robot inertia matrix, and $N(q, \dot{q})$ is the $(nx1)$ vector of centrifugal, Coriolis, gravitational and friction forces/torques.

The choice of the modified Denavit and Hartenberg frames attached to each link allows to obtain a dynamic model linear in relation to a set of standard dynamic parameters, χ_{st} (Gautier 1986), (Gautier et W. Khalil 1990):

$$\tau_{idm} = IDM_{st}(q, \dot{q}, \ddot{q}) \chi_{st} \quad (2)$$

Where $IDM_{st}(q, \dot{q}, \ddot{q})$, is the (nxN_s) jacobian matrix of τ_{idm} , with respect to the $(N_s \times 1)$ vector χ_{st} , of the standard parameters given by:

$$\chi_{st} = \begin{bmatrix} \chi_{st}^{1T} & \chi_{st}^{2T} & \dots & \chi_{st}^{nT} \end{bmatrix}^T \quad (3)$$

With:

$$\chi_{sj} = [XX_j \ XY_j \ XZ_j \ YY_j \ YZ_j \ ZZ_j \ MX_j \ MY_j \ MZ_j \ M_j \ I a_j \ Fv_j \ Fc_j \ \tau_{offj}]^T,$$

where:

- $XX_j, XY_j, XZ_j, YY_j, YZ_j, ZZ_j$, are the six components of the inertia matrix, ${}^j J_j$, of link j at the origin of frame j ,
- MX_j, MY_j, MZ_j , are the components of the first moments, ${}^j MS_j$, of link j ,
- M_j is the mass of link j ,
- $I a_j$, is a total inertia moment for rotor and gears of actuator j .
- Fv_j, Fc_j , are the viscous and Coulomb friction parameters of joint j .
- $\tau_{offj} = Of_{Fsj} + Of_{ij}$, is an offset parameter where Of_{Fsj} is the dissymmetry of the Coulomb friction with respect to the sign of the velocity and Of_{ij} is due to the current amplifier offset which supplies the motor.
- $N_s = 14 \times n$, is the number of standard parameters.

The base parameters are the minimum number of dynamic parameters from which the dynamic model can be calculated. They are obtained from the standard inertial parameters by eliminating those which have no effect on the dynamic model, and by regrouping some others by means of linear relations. They can be determined using simple closed-form rules (Gautier et W. Khalil 1990) or using a numerical method based on the QR decomposition (Gautier 1991).

The minimal inverse dynamic model can be written as:

$$\tau_{idm} = IDM(q, \dot{q}, \ddot{q}) \chi \quad (4)$$

Where:

$IDM(q, \dot{q}, \ddot{q})$, is the $(n \times b)$ matrix of the minimal set of basis functions of the rigid body dynamics, (5)

χ , is the $(b \times 1)$ vector of the b base parameters. (6)

Because of perturbations due to noise measurement and modeling errors, the actual force/torque τ differs from τ_{idm} , by an error e , such that:

$$\tau = \tau_{idm} + e = IDM(q, \dot{q}, \ddot{q}) \chi + e \quad (7)$$

Equation (7) gives the Inverse Dynamic Identification Model (IDIM).

We consider the off-line identification of the base dynamic parameters χ , given measured or estimated off-line data for τ and (q, \dot{q}, \ddot{q}) , collected while the robot is tracking some planned trajectories.

Usually, the signals available from the robot controller are the joint position measurement and the $(n \times 1)$ control signal vector v_c , calculated according to the control law.

Then (q, \dot{q}, \ddot{q}) in (7) are estimated with $(\hat{q}, \hat{\dot{q}}, \hat{\ddot{q}})$ respectively, obtained by bandpass filtering the measure of q (Gautier 1997). The derivatives are off-line calculated without phase shift, using a central difference algorithm of the lowpass filtered position \hat{q} . The filtered position \hat{q} is off-line calculated with a non causal zero-phase digital filter by processing the input data q , through a lowpass Butterworth filter in both the forward and reverse direction, using the `filtfilt` procedure from Matlab.

The control signal v_τ , is connected to the input current reference of the current closed-loop of the amplifiers which supplies the motors. Assuming that the current closed-loop has a large bandwidth, greater than 500Hz, its transfer function is equal to its static gain, K_c , in the frequency range (less than 10Hz) of the rigid robot dynamics. Then, the actual force/torque τ , is calculated with the relation:

$$\tau = g_\tau v_\tau \quad (8)$$

where:

g_τ , is the $(n \times n)$ diagonal matrix of the drive gains,

with:

$$g_\tau = K_r K_c K_\tau \quad (9)$$

where:

- K_r , is the $(n \times n)$ gear ratios diagonal matrix of the joint drive chains ($\dot{q}_m = K_r \dot{q}$, with \dot{q}_m , the velocity on the motor side),
- K_c , is the $(n \times n)$ static gains diagonal matrix of the current amplifiers,
- K_τ , is the $(n \times n)$ diagonal matrix of the electromagnetic motor torque constants.
- Those parameters have a priori values, given by manufacturers, which can be checked with special tests (Restrepo et Gautier 1995).

The inverse dynamic identification model (IDIM) (7) is calculated at a frequency measurement f_m , using samples of $(\hat{q}, \hat{\dot{q}}, \hat{\ddot{q}})$ to calculate $IDM(\hat{q}, \hat{\dot{q}}, \hat{\ddot{q}})$ and samples of v_τ to calculate τ with (8), at different times t_k , $k = 1, \dots, n_m$, while the robot is tracking a reference trajectory $(q_r, \dot{q}_r, \ddot{q}_r)$, during the time length T_{obs} , of the trajectory.

The equations of each joint are regrouped together on all the trajectory to get an over-determined linear system such that:

$$Y_{fm}(\tau) = W_{fm}(\hat{q}, \hat{\dot{q}}, \hat{\ddot{q}}) \chi + \rho_{fm} \quad (10)$$

With:

$$Y_{fm}(\tau) = \begin{bmatrix} Y_{fm}^1 \\ \dots \\ Y_{fm}^n \end{bmatrix}, Y_{fm}^j = \begin{bmatrix} \tau_j(t_1) \\ \dots \\ \tau_j(t_{n_m}) \end{bmatrix} \quad (11)$$

$$W_{fm}(\hat{q}, \hat{\dot{q}}, \hat{\ddot{q}}) = \begin{bmatrix} W_{fm}^1 \\ \dots \\ W_{fm}^n \end{bmatrix}, W_{fm}^j = \begin{bmatrix} IDM^j(\hat{q}(t_1), \hat{\dot{q}}(t_1), \hat{\ddot{q}}(t_1)) \\ \dots \\ IDM^j(\hat{q}(t_{n_m}), \hat{\dot{q}}(t_{n_m}), \hat{\ddot{q}}(t_{n_m})) \end{bmatrix} \quad (12)$$

where:

$IDM^j(\hat{q}(t_k), \hat{\dot{q}}(t_k), \hat{\ddot{q}}(t_k))$, is the j th row of the $(n \times b)$ regressor matrix $IDM(\hat{q}(t_k), \hat{\dot{q}}(t_k), \hat{\ddot{q}}(t_k))$, (5).

Y_{fm}^j and W_{fm}^j , represent the n_m equations of joint j , $n_m = T_{obs} * f_m$, is the number of sample measurements.

The notation $W_{fm}(IDM(\hat{q}, \hat{\dot{q}}, \hat{\ddot{q}})) = W_{fm}(\hat{q}, \hat{\dot{q}}, \hat{\ddot{q}})$ will be used also to recall that W_{fm} , is calculated with a sampling of $IDM(\hat{q}, \hat{\dot{q}}, \hat{\ddot{q}})$.

In order to eliminate high frequency force/torque ripple in τ , and to window the identification frequency range into the model dynamics, a parallel decimation procedure low-pass filters in parallel Y_{fm} and each column of W_{fm} and resamples them at a lower rate, keeping one sample over n_d . This parallel decimation can be carried out with the Matlab `decimate` function, where the lowpass filter cut-off frequency is equal to $0.8 \times f_m / (2 \times n_d)$.

After the data acquisition procedure and the parallel decimation of (10), we obtain the over determined linear system:

$$Y(\tau) = W(\hat{q}, \hat{\dot{q}}, \hat{\ddot{q}}) \chi + \rho \quad (13)$$

where:

- $Y(\tau)$, is the $(r \times 1)$ vector of measurements, built from the actual force/torque τ ,
- $W(\hat{q}, \hat{\dot{q}}, \hat{\ddot{q}})$, is the $(r \times b)$ observation matrix, built from the estimated values $(\hat{q}, \hat{\dot{q}}, \hat{\ddot{q}})$ of (q, \dot{q}, \ddot{q}) .
- ρ , is the $(r \times 1)$ vector of errors.
- $r = n * n_m / n_d$, is the number of rows in (13).

In Y and W , the equations of each joint are grouped together such that:

$$Y = \begin{bmatrix} Y^1 \\ \dots \\ Y^n \end{bmatrix}, W = \begin{bmatrix} W^1 \\ \dots \\ W^n \end{bmatrix} \quad (14)$$

where Y^j and W^j represent the n_m / n_d equations of joint j .

The ordinary LS (OLS) solution $\hat{\chi}$ minimizes the

squared 2-norm $\|\rho\|^2$ of the vector of errors.

Using the base parameters and tracking “exciting” reference trajectories (Gautier et W. Khalil 1992) allow to get a full rank and well conditioned matrix W . The LS solution $\hat{\chi}$ is given by:

$$\hat{\chi} = \left((W^T W)^{-1} W^T \right) Y = W^+ Y \quad (15)$$

It is computed using the QR factorization of W . Standard deviations $\sigma_{\hat{\chi}_i}$, are estimated using classical results from statistics under the assumptions that W is a deterministic matrix, thanks to the data filtering procedure described above, and ρ , is a zero-mean additive independent Gaussian noise, with a covariance matrix $C_{\rho\rho}$, such that:

$$C_{\rho\rho} = E(\rho\rho^T) = \sigma_\rho^2 I_r \quad (16)$$

where E is the expectation operator and I_r , the (rxr) identity matrix.

An unbiased estimation of the standard deviation σ_ρ is:

$$\hat{\sigma}_\rho^2 = \|Y - W\hat{\chi}\|^2 / (r - b) \quad (17)$$

The covariance matrix of the estimation error is given by:

$$C_{\hat{\chi}\hat{\chi}} = E[(\chi - \hat{\chi})(\chi - \hat{\chi})^T] = \hat{\sigma}_\rho^2 (W^T W)^{-1} \quad (18)$$

$\sigma_{\hat{\chi}_i}^2 = C_{\hat{\chi}\hat{\chi}}(i, i)$ is the i^{th} diagonal coefficient of $C_{\hat{\chi}\hat{\chi}}$. The relative standard deviation $\% \sigma_{\hat{\chi}_i}$ is given by:

$$\% \sigma_{\hat{\chi}_i} = 100 \sigma_{\hat{\chi}_i} / |\hat{\chi}_i|, \text{ for } |\hat{\chi}_i| \neq 0 \quad (19)$$

The OLS can be improved by taking into account different standard deviations on joint j equations errors (Gautier 1997). Each equation of joint j in (13), (14), is weighted with the inverse of the standard deviation of the error calculated from OLS solution of the equations of joint j , given by:

$$Y^j(\tau_j) = W^j \left(IDM^j(\hat{q}, \hat{\dot{q}}, \hat{\ddot{q}}) \right) \chi + \rho^j \quad (20)$$

This weighting operation normalizes the errors in (13) and gives the weighted LS (WLS) estimation of the parameters.

This identification method is illustrated in Fig. 1. The calculation of the velocities and accelerations are required using well tuned bandpass filtering of the joint position (Gautier 1997).

One of the numerous validations of the identification is to simulate, a posteriori, the direct dynamic model (DDM) given by (10) and to compare the simulated trajectories with real trajectories when the torques are the same. These comparisons have to be done on trajectories which were not used for the identification process.

$$\ddot{q} = M^{-1}(q)(\tau - N(q, \dot{q})) \quad (21)$$

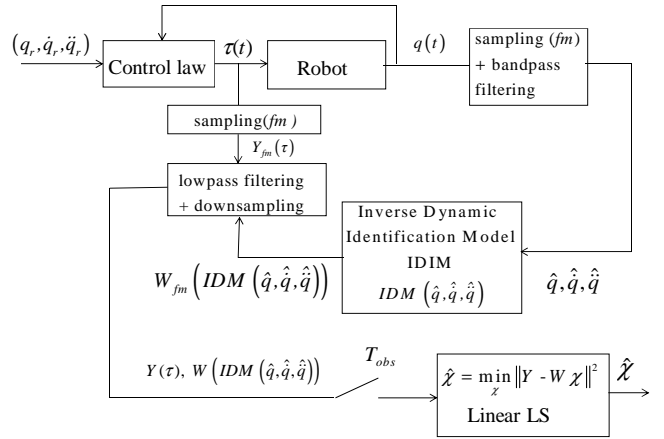


Fig. 1: IDIM LS identification scheme.

3. Instrumental variable technique

3.1. Theoretical approach

From a theoretical point of view, the statistical assumptions for efficient LS estimation are violated in practical applications. In the equation (13), the observation matrix W is built from the measured joint positions q and from \dot{q} , \ddot{q} , which are numerically computed from q , \dot{q} , \ddot{q} . Therefore the observation matrix is noisy. Moreover identification is carried out in closed-loop control. These violations of assumption imply that the LS estimator, $\hat{\chi}$, may be non consistent. Indeed, from (13), it comes:

$$W^T Y = W^T W \chi + W^T \rho_{ev} = W^T W \hat{\chi} \quad (22)$$

With ρ_{ev} is the vector of errors (errors in variable) when W is corrupted by noise $W = W_{nf} - \Delta W$

$$\rho_{ev} = \Delta W \chi + \rho \quad (23)$$

Thanks to the Slutsky's theorem, it is obtained:

$$\text{plim}_{m \rightarrow \infty} \hat{\chi} = \chi + \text{plim}_{m \rightarrow \infty} \left(\frac{1}{m} W_m^T W_m \right)^{-1} \text{plim}_{m \rightarrow \infty} \left(\frac{1}{m} W_m^T \rho_{evm} \right) \quad (24)$$

With:

plim is the convergence in probability,

m is the number of repetition of W and ρ_{ev} ,

W_m (resp. ρ_{evm}) is the concatenation of W (resp. ρ_{ev}).

Under the classical assumptions:

$$\text{plim}_{m \rightarrow \infty} \left(\frac{1}{m} W_m^T W_m \right) = E(W^T W) \text{ is positive definite} \quad (25)$$

$$\text{plim}_{m \rightarrow \infty} \left(\frac{1}{m} W_m^T \rho_{evm} \right) = E(W^T \rho_{ev}) \text{ exists} \quad (26)$$

As ρ_{ev} depends on the observation matrix W according to (23), $E(W^T \rho) \neq 0$. Therefore, the estimator is not consistent.

Instrumental Variable method deals with this problem of noisy observation matrix (called error in variable in the statistical frame) and can be statistically optimal (Davidson et Mackinnon 1993) (Young et Jakeman 1979). The Instrumental Variable Method proposes a consistent estimator by building the instrument matrix V such as (22) becomes:

$$V^T Y = V^T W \chi + V^T \rho_{ev} = V^T W \hat{\chi}_V \quad (27)$$

The instrumental variable solution, $\hat{\chi}_V$, is the solution of (27):

$$\hat{\chi}_V = (V^T W)^{-1} V^T Y \quad (28)$$

In the following V is calculated as a function of $\hat{\chi}_V$. That defines an iterative procedure such as:

$$\hat{\chi}_{V_{k+1}} = (V_k^T W)^{-1} V_k^T Y \quad (29)$$

where : $V_k = V(\hat{\chi}_{V_k})$

This needs for $(V_k^T W)$ to be a regular matrix. Assuming:

$$\text{plim}_{m \rightarrow \infty} \left(\frac{1}{m} V_{k,m}^T W_m \right) \text{ is non singular and,} \quad (30)$$

$$\text{plim}_{m \rightarrow \infty} \left(\frac{1}{m} V_{k,m}^T \rho_{evm} \right) = E(V_k^T \rho_{ev}) = 0 \quad (31)$$

With $V_{k,m}$ is the concatenation of V_k

for any k , $\hat{\chi}_{V_k}$ converges to χ with m . Indeed, with the Slutsky's theorem, we obtain:

$$\text{plim}_{m \rightarrow \infty} \hat{\chi}_{V_k} = \chi + \text{plim}_{m \rightarrow \infty} \left(\frac{1}{m} V_{k,m}^T W_m \right)^{-1} \text{plim}_{m \rightarrow \infty} \left(\frac{1}{m} V_{k,m}^T \rho_{evm} \right) \quad (32)$$

And with (30) and (31), it comes:

$$\text{plim}_{m \rightarrow \infty} \hat{\chi}_{V_k} = \chi \quad (33)$$

Then the IV estimator is consistent.

3.2. Calculation of the instrumental matrix

The main problem is to find an instrument matrix V . A usual solution is to build an observation matrix from simulated data instead of measured data. These simulated data (called also instruments) are the outputs of an auxiliary model (Young et Jakeman 1979) which is an approximation of the noise-free model of the process to be identified. We chose the Direct Dynamic Model of the robot (DDM) given by (21) to be this auxiliary model.

The IV method adapted for dynamic identification of robots can be resumed by the following algorithm illustrated

Fig. 2:

- The algorithm is initialized with any the values according to the subsection 3.4.
- At each step of the iterative algorithm, $q_s, \dot{q}_s, \ddot{q}_s$ are calculated by simulation of the closed loop robot tracking exciting trajectories using the DDM with the parameters identified at the previous step. W_s is obtained as a sam-

pling of IDIM, $ID_s(q_s, \dot{q}_s, \ddot{q}_s)$, and we choose the instrument matrix as:

$$V_k(\hat{\chi}_{V_k}) = W_s(q_s, \dot{q}_s, \ddot{q}_s, \hat{\chi}_{V_k}) \quad (22)$$

$Y(\tau)$ is calculated from the sampling and filtering of the measurements of τ , and $W(q, \dot{q}, \ddot{q})$ is calculated through IDIM using the sampling and filtering of q .

- $\hat{\chi}_{V_{k+1}}$ is given by (29) which is the LS solution of

$$\frac{\|\hat{\epsilon}_{k+1}\| - \|\hat{\epsilon}_k\|}{\|\hat{\epsilon}_k\|} \leq \alpha$$

(27),

- The algorithm stops when the relative error decreases under a tolerance, ideally chosen to be a small number):

with the estimation error:

$$\epsilon_k = Y - W_s \hat{\chi}_{V_k}$$

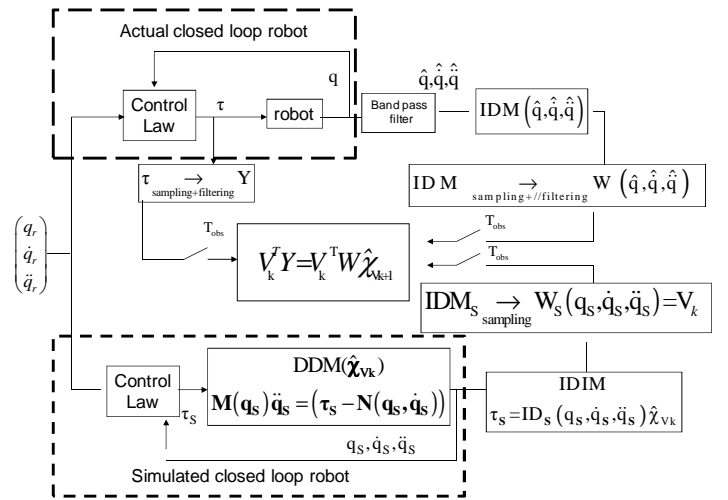


Fig. 2 : IV identification procedure

3.3. Calculation of the solution

Suitable solutions consist in using orthogonal projection such as QR decomposition. In this case, we have:

$$W = Q_W R_W,$$

$$V = Q_V R_V.$$

With:

Q_V and Q_W are orthogonal matrices which are projectors on the vectorial subspace spanned by the columns of V and W .

R_V and R_W are upper triangular matrices.

Considering only the b base parameters to be identified, we check we have at each iteration:

$$\text{rank}(R_W) = \text{rank}(Q_W) = \text{rank}(R_V) = \text{rank}(Q_V) = b.$$

This relation guarantees that the matrix $V^T W$ is invertible. Then, equation (27) becomes:

$$Q_V^T Y = Q_V^T Q_W R_W \chi + Q_V^T \rho_{ev} = Q_V^T Q_W R_W \hat{\chi}_V \quad (34)$$

$\hat{\chi}_V$ is the LS solution of the last equations.

Compared with LS regressions, the IV method needs two QR decompositions.

3.4. Initialization of the algorithm

Another problem is to choose the initial values $\hat{\chi}^0$.

We can use CAD values, or identified values with the IDIM method, but we show that there is no need at all of a priori values.

We propose an algorithm not sensitive to the initial conditions, which assumes that the condition

$$(q_{ddm}(\hat{\chi}_k), \dot{q}_{ddm}(\hat{\chi}_k), \ddot{q}_{ddm}(\hat{\chi}_k)) \square (q, \dot{q}, \ddot{q}) \quad (35)$$

is satisfied at any iteration k , and especially for $k=0$.

This is possible by taking the same control law structure for the actual robot and for the simulated one with the same performances given by the bandwidth, the stability margin or the closed-loop poles. Because the simulated robot parameters $\hat{\chi}^k$, change at each iteration k , the gains of the simulated control law must be updated according to $\hat{\chi}^k$.

For example, let us consider a PD control law for each joint j . The inverse dynamic model IDM (1) for the joint j , can be written as a decoupled double integrator perturbed by a coupling force/torque, such that:

$$\tau_j = \tau_{idm_j} = \sum_{i=1}^n M_{j,i}(q) \ddot{q}_i + N_j(q, \dot{q}) \quad (36)$$

$$= M_{j,j}(q) \ddot{q}_j + \sum_{i \neq j}^n M_{j,i}(q) \ddot{q}_i + N_j(q, \dot{q}) = M_{j,j}(q) \ddot{q}_j - p_j$$

where p_j is considered as a perturbation given by:

$$p_j = -\sum_{i \neq j}^n M_{j,i}(q) \ddot{q}_i - N_j(q, \dot{q}) \quad (37)$$

$M_{j,i}(q)$, which depends on q , is approximated by a constant inertia moment J_j , given by:

$$J_j = ZZ_j + I_{a_j} + \max(M_{j,j}(q) - ZZ_j - I_{a_j}) \quad (38)$$

J_j , is the maximum value, with respect to q , of the inertia moment around joint z_j axis. This gives the smallest damping value and the smallest stability margin of the closed-loop second order transfer function (42), while q varies.

It can be calculated from a priori CAD values of inertial parameters and must be taken at least as $ZZ_j + I_{a_j}$.

The joint j dynamic model is approximated by a double integrator, where p_j , is a perturbation, as following:

$$\ddot{q}_j = \frac{1}{M_{j,j}(q)} (\tau_j + p_j) \square \frac{1}{J_j} (\tau_j + p_j) \quad (39)$$

Let us consider the joint j PD control of the actual robot which is illustrated Fig. 3:

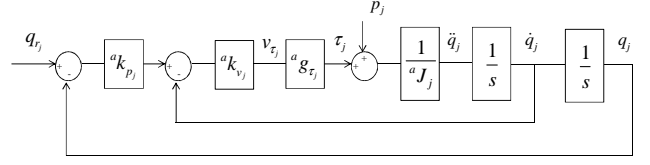


Fig. 3: Joint PD control of the actual robot.

The control input calculated by the robot controller is given by:

$$v_{\tau_j} = {}^a k_{p_j} {}^a k_{v_j} (q_{r_j} - q_j) - {}^a k_{v_j} \dot{q}_j \quad (40)$$

v_{τ_j} , is the current reference of the current amplifiers which supplies the motor.

The joint j , force/torque is given by:

$$\tau_j = {}^a g_{\tau_j} v_{\tau_j} \quad (41)$$

where:

${}^a g_{\tau_j}$, is the actual drive gain, calculated with the actual parameters in (9).

${}^a J_j$, is the actual value of J_j .

In order to tune the tracking performances of the reference position q_{r_j} , the transfer function $\frac{q_{r_j}}{q_j}$ is calculated with $p_j=0$:

$$H_j = \left(\frac{q_j}{q_{r_j}} \right)_{p_j=0} = \frac{1}{\frac{{}^a J_j s^2}{{}^a g_{\tau_j} {}^a k_{v_j} {}^a k_{p_j}} + \frac{1}{{}^a k_{p_j}} s + 1} \quad (42)$$

$$H_j = \left(\frac{q_j}{q_{r_j}} \right)_{p_j=0} = \frac{1}{\frac{s^2}{{}^a \omega_{nj}^2} + \frac{2 {}^a \zeta_j}{{}^a \omega_{nj}} s + 1}$$

where:

${}^a \omega_{nj}$, is the actual natural frequency which characterizes the closed-loop bandwidth,

${}^a \zeta_j$, is the actual damping coefficient which characterizes the closed-loop stability margin, with:

$${}^a \omega_{nj} = \sqrt{{}^a k_{p_j} {}^a k_{v_j} \frac{{}^a g_{\tau_j}}{{}^a J_j}}, \quad {}^a \zeta_j = \frac{1}{2} \sqrt{\frac{{}^a k_{v_j} {}^a g_{\tau_j}}{{}^a k_{p_j} {}^a J_j}} \quad (43)$$

Then it comes:

$${}^a k_{p_j} = \frac{{}^a \omega_{nj}^2}{2 {}^a \zeta_j^2}, \quad {}^a k_{v_j} = 2 {}^a \zeta_j {}^a \omega_{nj} \frac{{}^a J_j}{{}^a g_{\tau_j}} \quad (44)$$

The closed-loop performances are chosen with the desired 2 poles of a second order transfer function characterized by, ${}^d\omega_{nj}$, ${}^d\zeta_j$, where:

${}^d\omega_{nj}$, is the desired natural frequency,

${}^d\zeta_j$, is the desired damping coefficient.

Because the actual values are unknown, the gains are calculated from (44), where the unknown actual values, ${}^a\omega_{nj}$, ${}^a\zeta_j$, aJ_j , ${}^ag_{i_j}$, are replaced respectively by their desired values, ${}^d\omega_{nj}$, ${}^d\zeta_j$, and by their a priori values,

${}^{ap}J_j$, ${}^{ap}g_{\tau_j}$:

$${}^ak_{p_j} = \frac{{}^d\omega_{nj}}{2{}^d\zeta_j}, \quad {}^ak_{v_j} = 2{}^d\zeta_j{}^d\omega_{nj} \frac{{}^{ap}J_j}{{}^{ap}g_{\tau_j}} \quad (45)$$

where:

${}^{ap}J_j$ and ${}^{ap}g_{\tau_j}$ are a priori values of the actual unknown values aJ_j and ${}^ag_{\tau_j}$, respectively.

Now, let us consider the joint j PD control of the simulated robot which is illustrated Fig. 4.

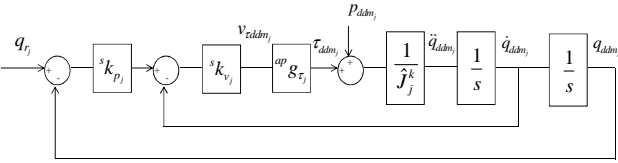


Fig. 4: Joint PD control of the simulated robot.

The variables $(v_{\tau ddm_j}, \tau_{ddm_j}, q_{ddm_j}, \dot{q}_{ddm_j}, \ddot{q}_{ddm_j})$, in Fig. 3, are computed by numerical integration of $DDM(\hat{\chi}^k)$, according to (21).

The control law of the simulated robot has the same structure as the actual one, Fig. 3, where we take:

${}^ag_{i_j} = {}^{ap}g_{i_j}$, the a priori value of ${}^ag_{i_j}$,

${}^aJ_j = \hat{J}_j^k$, the value of J_j , (38), calculated with the estimation $\hat{\chi}^k$, at iteration k .

${}^sk_{p_j}$, ${}^sk_{v_j}$, are the gains of the simulated control law.

They are calculated in order to keep the same performances for the simulated closed-loop and for the actual closed-loop, that is to say to keep the same desired values, ${}^d\omega_{nj}$ and ${}^d\zeta_j$, for the closed-loop poles. Then, it comes:

$${}^sk_{p_j} = \frac{{}^d\omega_{nj}}{2{}^d\zeta_j} = {}^ak_{p_j}, \quad {}^sk_{v_j} = 2{}^d\zeta_j{}^d\omega_{nj} \frac{\hat{J}_j^k}{{}^{ap}g_{\tau_j}} \quad (46)$$

The proportional gain, ${}^sk_{p_j}$, does not depend at all on the parameters values, but the derivative gain in the simu-

lator, ${}^sk_{v_j}$, must be updated with \hat{J}_j^k , at each iteration k .

It is important to note that only the gain in the simulated closed-loop, ${}^sk_{v_j}$, is modified during the iterative procedure. The actual gain of the robot control law, ${}^ak_{v_j}$, is not modified.

The simulated closed-loop tuning given by, ${}^d\omega_{nj}$, ${}^d\zeta_j$, differs from the actual one, ${}^a\omega_{nj}$, ${}^a\zeta_j$, with the following ratio, calculated by taking (45) into (43):

$$\frac{{}^a\omega_{nj}}{{}^d\omega_{nj}} = \frac{{}^a\zeta_j}{{}^d\zeta_j} = \sqrt{\frac{{}^{ap}J_j{}^ag_{\tau_j}}{{}^aJ_j{}^{ap}g_{\tau_j}}} \quad (47)$$

Usually this ratio is between 0.8 and 1.2. The actual values, ${}^a\omega_{nj}$, ${}^a\zeta_j$, can be estimated from step response or frequency analysis of the actual closed-loop. But this is not necessary, because there is little effect on the identification accuracy, assuming, ${}^d\omega_{nj}$, is regularly chosen more than 10 times greater than the frequency range of the robot dynamics. This allows to keep $(q_{ddm}(\hat{\chi}_k), \dot{q}_{ddm}(\hat{\chi}_k), \ddot{q}_{ddm}(\hat{\chi}_k)) \square (q, \dot{q}, \ddot{q})$, at each iteration k .

We propose to take a regular inertia matrix $M(q_{ddm}, \hat{\chi}^0)$, in order to have a good initialization for the numerical integration of the DDM given by (21). This is named the "regular initialization".

It can be obtained with:

$$\hat{\chi}^0 = 0, \text{ except for, } Ia_j^0 = 1, j = 1, n \quad (48)$$

The inertia of the rotor and gear of actuator j is generally taken into account in the IDM model (1) as:

$$\tau_{r_j} = Ia_j \ddot{q}_j \quad (49)$$

Then, the initial inertia matrix becomes the identity matrix, which is the best regular matrix:

$$M(q_{ddm}, \hat{\chi}^0) = I_n \quad (50)$$

Another simple regular initialization is to take:

$$\hat{\chi}^0 = 0, \text{ except for, } ZZ_j^0 = 1, j = 1, n \quad (51)$$

The initial inertia matrix, $M(q_{ddm}, \hat{\chi}^0)$, is no more the identity matrix, but remains regular.

Another point is to choose the state initial condition of the state vector, $(q_{ddm}(0), \dot{q}_{ddm}(0))$, in order to integrate the DDM. The actual values $(q(0), \dot{q}(0))$, are supposed to be not perfectly known because of noises. Then, we choose, $(q_{ddm}(0), \dot{q}_{ddm}(0)) = (q_r(0), \dot{q}_r(0))$, which is close to $(q(0), \dot{q}(0))$. Because the closed-loop transient response due to different initial conditions differs between the actual and the simulated signals during a transient period of approximately, $5/{}^d\omega_n$, the corresponding joint force/torque samples are eliminated from the identification data.

3.5. Discussion on the assumptions

The IV method is based on two assumptions. The instruments matrix has to be not correlated with the noise (see (31)) and the matrices product between the instrument matrix and the noisy observation matrix has to be full rank (see (30)). These two assumptions imply that the IV estimator is consistent.

As seen in the previous section, the instrument matrix is built from a deterministic simulation. The only link between the instrument and the noise could be provided indirectly from the parameters identified at the previous step. This correlation is much lower than the noise on the system. Assuming that ρ_{ev} is a zero-mean additive independent noise, we have:

$$E(V_k^T \rho_{ev}) \square E(V_k^T) E(\rho_{ev}) = 0$$

Which guarantees the assumption (31).

In this paper, it is assumed that the trajectory is enough exciting in order to identify the base parameters. This means that : $W_{nf}(q, \dot{q}, \ddot{q})$ which is the noise free observation matrix built from the real trajectory, is full rank. According to the last section:

$$(q_{ddm}(\hat{\chi}_k), \dot{q}_{ddm}(\hat{\chi}_k), \ddot{q}_{ddm}(\hat{\chi}_k)) \square (q, \dot{q}, \ddot{q}) \text{ so } V_k \square W_{nf}.$$

As $W \square W_{nf} - \Delta W$, it comes $V_k^T W = W_{nf}^T W_{nf} - W_{nf}^T \Delta W$

It is not very probable that the noise on the observation matrix ΔW gives the assumed full rank matrix $V_k^T W$ singular. Indeed, we collect a very high number of samplings (at least 500 x b). So, the noises tend to be zero-mean additive independent noises. It means the columns of ΔW are independent. ΔW is also a full rank matrix. In addition, we check we obtain $\text{rank}(R_W) = \text{rank}(R_V) = \text{rank}(Q_W) = \text{rank}(Q_V) = b$ at each step of the algorithm. Therefore, the assumption (30) is always true.

4. Experimental Validation

4.1. Case study: modeling of the SCARA robot

The identification method is carried out on a 2 degrees of freedom planar direct drive prototype robot without gravity effect, shown on Fig. 5. This direct drive prototype is very well suited to our purpose because it emphasizes non linear coupling when classical industrial robots with gear ratio above 50, divides this non-linear phenomenon by at least 2500. Moreover, the dynamic model of this robot includes eight parameters which allows us to present several conditions for the identification. At last, this robot and its real parameters, called the nominal parameters, are well known. Thus, we can check the physical meaning of the identified parameters.

The description of the geometry of the robot uses the modified Denavit and Hartenberg (DHM) notations (W.

Khalil et Kleinfinger 1986) which are illustrated on Fig. 6. The robot is direct driven by 2 DC permanent magnet motors supplied by PWM amplifiers.



Fig. 5: The scara robot prototype.

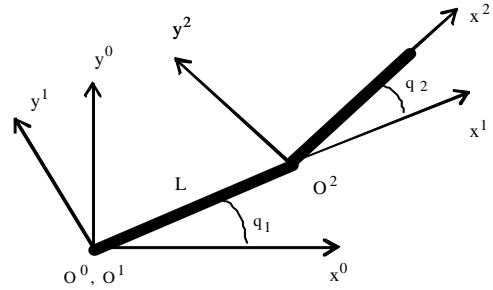


Fig. 6: DHM frames of the scara robot.

The dynamic model depends on 8 minimal dynamic parameters, considering 4 friction parameters:

$$\mathcal{X} = [ZZ_{1R} \quad Fv_1 \quad Fc_1 \quad ZZ_{2R} \quad LMX_2 \quad LMY_2 \quad Fv_2 \quad Fc_2]^T \quad (52)$$

$$ZZ_{1R} = ZZ_1 + Ia_1 + M_2 L^2$$

$$ZZ_{2R} = ZZ_2 + Ia_2$$

$L = 0.5\text{m}$, is the length of the first link.

In the case of the SCARA robot, the parameters, LMX_2 , and LMY_2 , are identified instead of, MX_2 , and MY_2 , respectively.

The 8 columns, $IDM_{:,k}$, $k = 1,8$, of $IDM(q, \dot{q}, \ddot{q})$, in IDIM (7), are the following:

$$\begin{aligned}
IDM_{:,1} &= IDM_{ZZ_{1R}} = \begin{bmatrix} \ddot{q}_1 \\ 0 \end{bmatrix}, \quad IDM_{:,2} = IDM_{Fv_1} = \begin{bmatrix} \dot{q}_1 \\ 0 \end{bmatrix}, \\
IDM_{:,3} &= IDM_{Fc_1} = \begin{bmatrix} \text{sign}(\dot{q}_1) \\ 0 \end{bmatrix}, \quad IDM_{:,4} = IDM_{ZZ_{2R}} = \begin{bmatrix} \ddot{q}_1 + \ddot{q}_2 \\ \ddot{q}_1 + \ddot{q}_2 \end{bmatrix}, \\
IDM_{:,5} &= IDM_{LMX_2} = \begin{bmatrix} (2\ddot{q}_1 + \ddot{q}_2) \cos q_2 - \dot{q}_2 (2\dot{q}_1 + \dot{q}_2) \sin q_2 \\ \ddot{q}_1 \cos q_2 + \dot{q}_1^2 \sin q_2 \end{bmatrix}, \\
IDM_{:,6} &= IDM_{LMY_2} = \begin{bmatrix} -(2\ddot{q}_1 + \ddot{q}_2) \sin q_2 - \dot{q}_2 (2\dot{q}_1 + \dot{q}_2) \cos q_2 \\ \dot{q}_1^2 \cos q_2 - \ddot{q}_1 \sin q_2 \end{bmatrix}, \\
IDM_{:,7} &= IDM_{Fv_2} = \begin{bmatrix} 0 \\ \dot{q}_2 \end{bmatrix}, \quad IDM_{:,8} = IDM_{Fc_2} = \begin{bmatrix} 0 \\ \text{sign}(\dot{q}_2) \end{bmatrix}
\end{aligned} \tag{53}$$

The closed-loop control is a PD control law (40), according to Fig. 3, with:

$$J_1 = ZZ_{1R} + ZZ_{2R} + 2 LMX_2, \text{ and } J_2 = ZZ_{2R}.$$

The actual gains are calculated with (45), taking a desired damping, ${}^d\zeta_j=1$, for joint 1 and joint 2.

The desired natural frequency, ${}^d\omega_{nj}$, is chosen according to the driving capacity without saturation of the joint drive. For this robot we obtain a full bandwidth with, ${}^d\omega_{n_1}^f = 1rd/s$, and ${}^d\omega_{n_2}^f = 10rd/s$.

The sample rates of the control and of the measurement are equal to, $f_m=200\text{Hz}$.

Torque data are obtained from (41), and from the current reference data v_τ .

The simulation of the robot is carried out with the same reference trajectory and with the same control law structure as the actual robot.

The gains in the simulator are calculated with (46) and with the same values, ${}^d\zeta_j=1$, ${}^d\omega_{n_1}^f = 1rd/s$, and ${}^d\omega_{n_2}^f = 10rd/s$.

The new identification process is performed in different cases in order to compare the previous IDIM technique to the new IV technique and to investigate the robustness of IV with respect to the initialization, to the data filtering and to the closed-loop tuning. All the results are given in SI units, on the joint side.

4.2. Comparison of IDIM and IV with good initial values, $\hat{\chi}^0 = \hat{\chi}^{IV}$.

At first, the algorithm is initialized with, $\hat{\chi}^{IDIM}$, the vector of parameters identified with the IDIM LS estimator.

The IDIM LS off-line estimation is carried out with a filtered position \hat{q} , calculated with a 20Hz cut-off frequency forward and reverse Butterworth filter, and with the velocities $\hat{\dot{q}}$, and the accelerations, $\hat{\ddot{q}}$, calculated with a central difference algorithm of \hat{q} . The parallel decima-

tion of Y_{fm} and W_{fm} , in (10), is carried out with a sample rate divided by a factor, $n_d=20$, and a lowpass filter cut-off frequency equal to, $0.8*f_m/(2*n_d)=4\text{Hz}$. The results of the IDIM identification are given in Table 1.

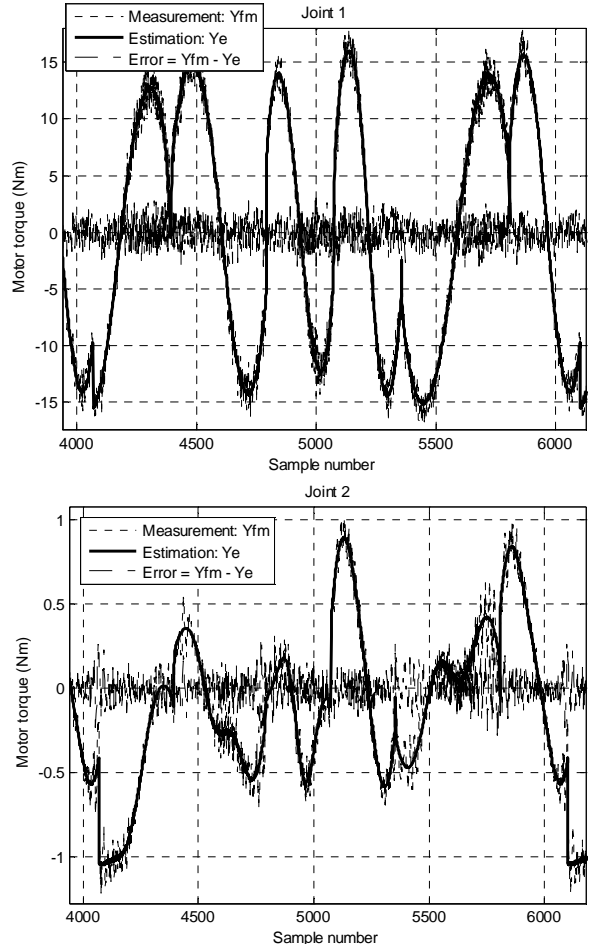
Starting with good initial values $\hat{\chi}^0 = \hat{\chi}^{IV}$, IV algorithms converges in only 2 steps to obtain the optimal solution as shown in the table 2. The IV solution is very close to the IDIM solution. Hence, the IV method does not improve the IDIM solution calculated with good bandpass filtered data.

A validation is plotted on Fig 7, at the frequency measurement, $f_m=200\text{Hz}$. It shows that the actual joint torques, $Y_{fm}(\tau)$, and the torques estimated with the identified model, $Y_e = W_{\delta_{fm}}(q_{ddm}, \dot{q}_{ddm}, \ddot{q}_{ddm}, \hat{\chi}^2) \hat{\chi}^2$ are very close.

Both methods give a small relative norm error, $\|Y - W\hat{\chi}\|/\|Y\| < 3\%$, which shows a good accuracy for the model and for the identified values.

It can be seen that the parameters, Fv_1 , and Fv_2 , have no significant estimations because of their large relative standard deviation ($>30\%$). They have no significant contribution in the joint torques and they can be cancelled to keep a set of essential parameters of a simplified dynamic model, without loss of accuracy (W. Khalil, Gautier, et Lemoine 2007).

However, we prefer to keep all the parameters in the following, for a better comparison of IDIM and IV identification methods.



LMX_2	0.0	0.124	0.0013	0.52
LMY_2	0.0	0.007	0.0005	3.5
Fv_2	0.0	0.013	0.0084	30.0
Fc_2	0.0	0.137	0.008	3.0

Fig. 7.IV validation

Table 1: IDIM identification

Parameter	$\hat{\chi}^{IDIM}$	$2 \sigma_{\hat{\chi}}$	$\% \sigma_{\hat{\chi}}$
ZZ_{IR}	3.44	0.034	0.50
Fv_1	0.03	0.031	52.0
Fc_1	0.82	0.1	6.0
ZZ_2	0.062	0.0006	0.51
LMX_2	0.121	0.0014	0.56
LMY_2	0.007	0.0007	5.0
Fv_2	0.013	0.006	23.0
Fc_2	0.137	0.006	2.30
$\ Y - W \hat{\chi}^{IDIM}\ / \ Y\ = 0.024$			

Table 2: IV identification

Parameter		$\hat{\chi}^2$	$2 \sigma_{\hat{\chi}}$	$\% \sigma_{\hat{\chi}}$
ZZ_{IR}	3.44	3.45	0.036	0.52
Fv_1	0.03	0.04	0.032	40.0
Fc_1	0.82	0.82	0.05	3.0
ZZ_2	0.062	0.061	0.0006	0.49
LMX_2	0.121	0.124	0.0013	0.52
LMY_2	0.007	0.007	0.0005	3.5
Fv_2	0.013	0.013	0.0084	30.0
Fc_2	0.137	0.137	0.008	3.0
$\ Y - W \hat{\chi}^{IV}\ / \ Y\ = 0.021$				

4.3. IV, validation of the regular initialization,

$$M(q_{ddm}, \hat{\chi}^0) = I_2.$$

The robustness of IV with respect to a wrong initialization, such as the regular initialization (50), is investigated.

The initial values of the dynamic parameters are given by (48), with:

$$\hat{\chi}^0 = [1 \ 0 \ 0 \ 1 \ 0 \ 0 \ 0 \ 0]^T$$

The identified values given in Table 3, are very close to those given in Table 1. This result validates the regular initialization procedure.

Moreover the algorithm converges in only 3 steps and is not time consuming.

Table 3: IV identification with regular initialization

Parameter	$\hat{\chi}^0$	$\hat{\chi}^3$	$2 \sigma_{\hat{\chi}}$	$\% \sigma_{\hat{\chi}}$
ZZ_{IR}	1.0	3.45	0.036	0.52
Fv_1	0.0	0.04	0.032	40.0
Fc_1	0.0	0.82	0.05	3.0
ZZ_2	1.0	0.061	0.0006	0.49

The relative norm errors on joint position, velocity and acceleration are plotted on Fig.8, with the following legend:

- norm error relative to the actual filtered joint position, $\|q_{ddm_j} - \hat{q}_j\| / \|\hat{q}_j\|$, velocity $\|\dot{q}_{ddm_j} - \hat{\dot{q}}_j\| / \|\hat{\dot{q}}_j\|$, and acceleration, $\|\ddot{q}_{ddm_j} - \hat{\ddot{q}}_j\| / \|\hat{\ddot{q}}_j\|$, where $(\hat{q}, \hat{\dot{q}}, \hat{\ddot{q}})$, are calculated as given in section 4.2.

- * norm error relative to the reference joint position, $\|q_{ddm_j} - q_{r_j}\| / \|q_{r_j}\|$, velocity, $\|\dot{q}_{ddm_j} - \dot{q}_{r_j}\| / \|\dot{q}_{r_j}\|$, and acceleration, $\|\ddot{q}_{ddm_j} - \ddot{q}_{r_j}\| / \|\ddot{q}_{r_j}\|$.

The assumption (35),

$(q_{ddm}(\hat{\chi}_k), \dot{q}_{ddm}(\hat{\chi}_k), \ddot{q}_{ddm}(\hat{\chi}_k)) \square (\hat{q}, \hat{\dot{q}}, \hat{\ddot{q}})$, at each iteration k , is confirmed Fig. 8, with a constant relative norm error close to 0.5% for the position, 5%, for the velocity and 10%, for the acceleration.

These results validate the updating procedure (46), of the simulated PD control law gains.

It can be seen also on Fig 8 that the simulated trajectory, $(q_{ddm}(\hat{\chi}_k), \dot{q}_{ddm}(\hat{\chi}_k), \ddot{q}_{ddm}(\hat{\chi}_k))$, is 3 to 5 times closer to the actual one, $(\hat{q}, \hat{\dot{q}}, \hat{\ddot{q}})$, than to the reference one,

$(q_r, \dot{q}_r, \ddot{q}_r)$, with a relative norm error close to 1.5% for the position, 15%, for the velocity and 30%, for the acceleration. Moreover, this error depends on the closed-loop bandwidth. It means that computing the observation matrix in (13) with the reference trajectory, $(q_r, \dot{q}_r, \ddot{q}_r)$, leads to a bad identification of the dynamic parameters.

Then, the assumption $(q_{ddm}(\hat{\chi}_k), \dot{q}_{ddm}(\hat{\chi}_k), \ddot{q}_{ddm}(\hat{\chi}_k)) \square (\hat{q}, \hat{\dot{q}}, \hat{\ddot{q}})$, is valid.

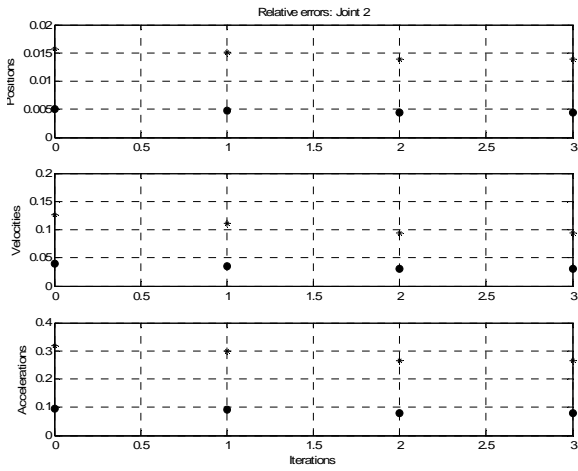
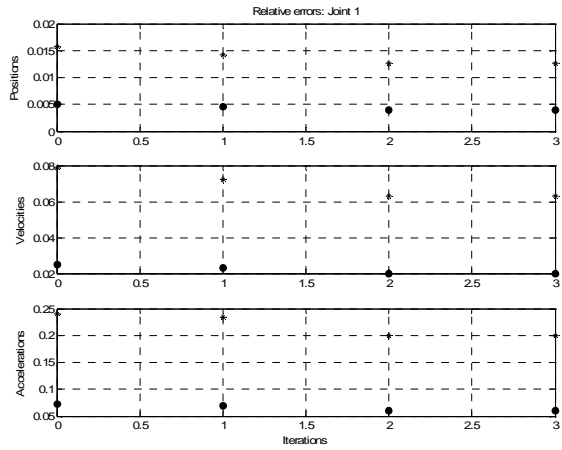


Fig. 8: • norm error relative to the filtered actual position, velocity, acceleration. * norm error relative to the reference position, velocity, acceleration.

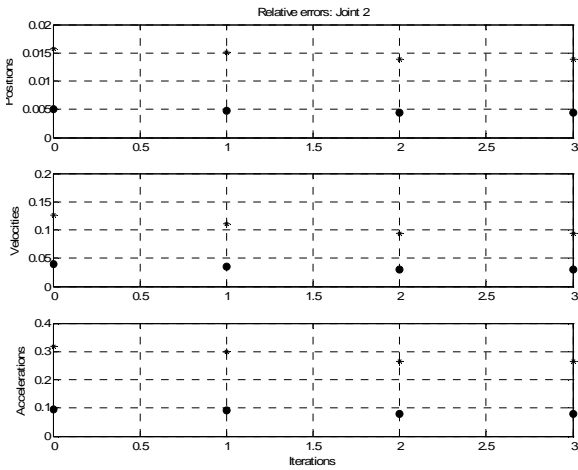


Fig. 9: • norm error relative to the filtered actual position, velocity, acceleration. * norm error relative to the reference position, velocity, acceleration.

The fast convergence of each parameter is shown in Table 4, and is plotted on Fig 10.

Table 4: Parameters convergence with IV identification

Parameter	$\hat{\chi}^0$	$\hat{\chi}^1$	$\hat{\chi}^2$	$\hat{\chi}^3$
ZZ_{IR}	1.0	3.46	3.45	3.45
FV_1	0.0	0.04	0.02	0.02
FC_1	0.0	0.82	0.85	0.85
ZZ_2	1.0	0.06	0.061	0.061
LMX_2	0.0	0.122	0.124	0.124
LMY_2	0.0	0.05	0.07	0.07
FV_2	0.0	0.005	0.01	0.01
FC_2	0.0	0.130	0.132	0.132

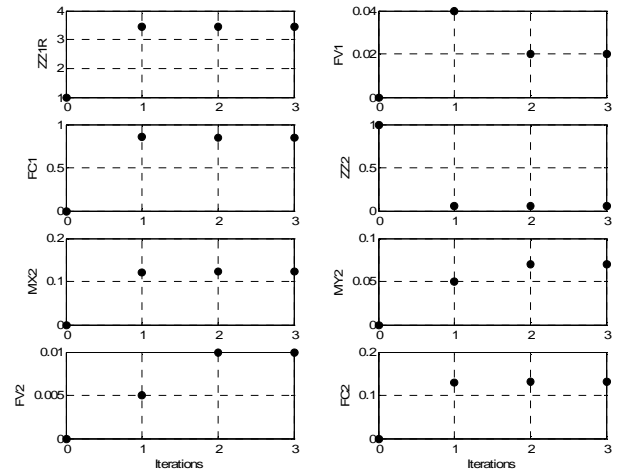


Fig. 10: IV parameters convergence

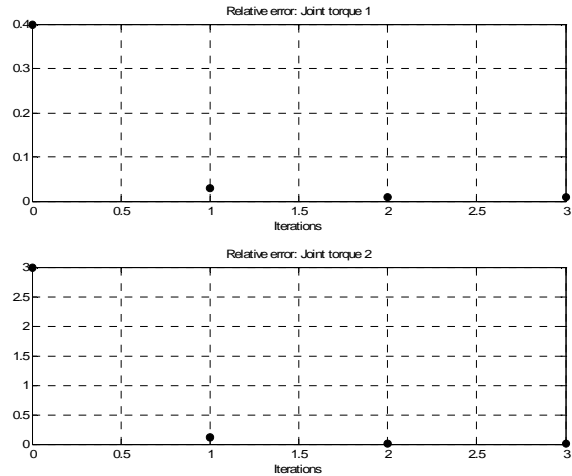


Fig. 11. IV, convergence of the joint torque error,

$$\|Y^j - W^j \hat{\chi}^k\| / \|Y^j\|$$

We have seen that $(q_{ddm}(\hat{\chi}_k), \dot{q}_{ddm}(\hat{\chi}_k), \ddot{q}_{ddm}(\hat{\chi}_k)) \square (\hat{q}, \hat{q}, \hat{q})$, at each iteration

k, with a constant small error. On the contrary, the relative torque norm error, given in Table 3, and plotted on Fig 12, dramatically decreases in only 3 steps. This shows the fast algorithm convergence.

4.4. Comparison of IDIM and IV, without data filtering.

All the actual and simulated data are sampled at $f_m = 200\text{Hz}$.

The IDIM LS estimation is carried out with the measured joint position q , and with $(\hat{q}, \hat{\dot{q}})$, calculated by a central difference algorithm of q , without lowpass Butterworth filtering. There is no parallel decimation. IDIM Results are given in Table 5

IV starts with the regular initialization. IV Results are given in Table 6.

Table 5: IDIM identification results without data filtering

Parameter	$\hat{\chi}^{IDIM}$	$2 \sigma_{\hat{\chi}}$	$\% \sigma_{\hat{\chi}}$
ZZ_{1R}	1.5	0.05	1.6
Fv_1	0.095	0.15	80.0
Fc_1	0.55	0.26	23.3
ZZ_2	0.14	0.018	6.7
LMX_2	0.63	0.035	2.7
LMY_2	0.1	0.023	11.8
Fv_2	0.001	0.143	700.0
Fc_2	0.19	0.244	68.40
$\ Y - W \hat{\chi}^{IDIM}\ / \ Y\ = 0.8$			

Table 6: IV identification results without data filtering

Parameter	$\hat{\chi}^0$	$\hat{\chi}^2$	$2 \sigma_{\hat{\chi}}$	$\% \sigma_{\hat{\chi}}$
ZZ_{1R}	1.0	3.45	0.007	0.1
Fv_1	0.0	0.05	0.023	21.0
Fc_1	0.0	0.81	0.004	0.24
ZZ_2	1.0	0.061	0.0004	0.3
LMX_2	0.0	0.124	0.0015	0.3
LMY_2	0.0	0.008	0.0009	5.6
Fv_2	0.0	0.023	0.0022	48.0
Fc_2	0.0	0.13	0.0038	1.5
$\ Y - W \hat{\chi}^{IDIM}\ / \ Y\ = 0.08$				

The identified values with IDIM are not good while the identified values with IV are still good.

IDIM fails because of the too large noise in the observation matrix, $W_{fm}(q, \hat{q}, \hat{\dot{q}})$, coming from the derivation of q , without lowpass filtering. Then the LS estimation is biased.

IV succeeds because the observation matrix, $W_{\delta fm}(q_{ddm}, \dot{q}_{ddm}, \ddot{q}_{ddm}, \hat{\chi}^k)$, is calculated without noise with the simulated values $(q_{ddm}, \dot{q}_{ddm}, \ddot{q}_{ddm})$.

This validation shows that IV cancels the bias of IDIM estimation, coming from a noisy estimation of $(\hat{q}, \hat{\dot{q}}, \hat{\ddot{q}})$, which gives a too noisy observation matrix $W_{fm}(q, \hat{q}, \hat{\dot{q}})$.

4.5. IV robustness with respect to error in the simulated closed-loop tuning, ${}^d \omega_n$

This section investigates the effect of an error between the actual value, ${}^a \omega_n$, and the simulated value ${}^d \omega_n$, of the natural frequency which represents the closed-loop bandwidth.

The IV identification is performed taking half the values of the full ones given in section 3.4, ${}^d \omega_{n_1} = {}^d \omega_{n_1}^f / 2 = 1/2$ (rd/s) and ${}^d \omega_{n_2} = {}^d \omega_{n_2}^f / 2 = 10/2$ (rd/s), and the same procedure used to obtain results shown in Table 2, that is to say a frequency measurement, $f_m = 200\text{Hz}$, and a parallel decimation with a factor, $n_d = 20$, and a lowpass filter cut-off frequency equal to 4Hz.

The parameters, given in Table 7, converge in only 6 steps to values which are very close to those obtained in Table 2, with a full closed-loop bandwidth.

Table 7: IV with half full bandwidth

Parameter	$\hat{\chi}^0$	$\hat{\chi}^6$	$2 \sigma_{\hat{\chi}}$	$\% \sigma_{\hat{\chi}}$
ZZ_{1R}	1.0	3.44	0.014	0.2
Fv_1	0.0	0.02	0.012	15.0
Fc_1	0.0	0.86	0.016	1.0
ZZ_2	1.0	0.060	0.0001	0.1
LMX_2	0.0	0.124	0.0002	0.1
LMY_2	0.0	0.007	0.0003	2.0
Fv_2	0.0	0.01	0.003	10.0
Fc_2	0.0	0.13	0.0008	0.3

The relative norm errors on joint position, velocity and acceleration are plotted on Fig 11, with the same legend as previously.

It can be seen that, $(q_{ddm}(\hat{\chi}_k), \dot{q}_{ddm}(\hat{\chi}_k), \ddot{q}_{ddm}(\hat{\chi}_k)) \square (\hat{q}, \hat{\dot{q}}, \hat{\ddot{q}})$, at each iteration k, with a constant norm error larger but close to the value obtained with the full bandwidth, Fig.11, close to, 0.5% for the position, 5%, for the velocity and 10%, for the acceleration.

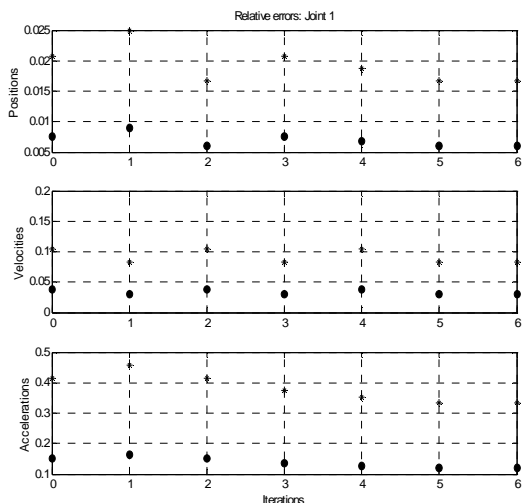


Fig. 12: ● norm error relative to the filtered actual position, velocity, acceleration. * norm error relative to the reference position, velocity, acceleration.

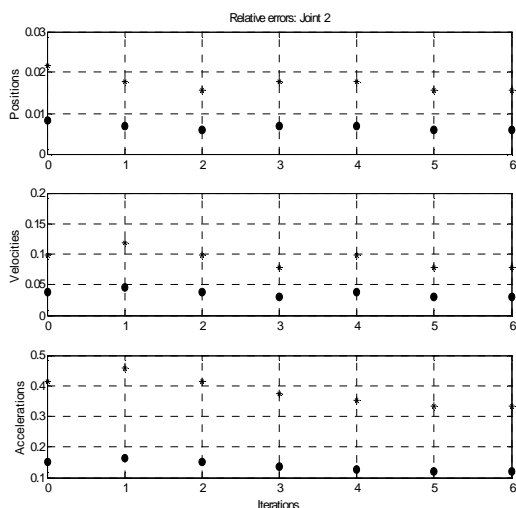


Fig. 13: ● norm error relative to the filtered actual position, velocity, acceleration. * norm error relative to the reference position, velocity, acceleration.

The relative torque norm error, given in Table 9, and plotted on Fig 12, decreases in 6 steps, only twice more than with the full bandwidth (see Table 3). This shows that IV is not very sensitive to error in the simulated closed-loop bandwidth, provided the control law structure is known.

However, IV fails beyond 1/3 of the full bandwidth, with ${}^d\omega_n \leq {}^d\omega_n^f / 3$.

5. Discussion and conclusion

One of the improvements of our algorithm is to avoid the acceleration calculation. It is one of the major difficult

points of the LS identification technique. In the general case, this problem is solved by a suitable data filtering. But, the choice of the cut-off frequency is crucial. If the cut-off frequency is too low the system is ill-conditioned and the main parameters are badly identified. On the other hand, if the cut-off frequency is too large, the observation matrix is strongly noisy and the LS estimator is biased. It is the reason why some techniques have been developed to overcome this problem: by integrating the dynamic model (Slotine et Weiping Li 1987)(Middleton et Goodwin 1988) or by using the power (Gautier 1997). The drawback of the method integrating the dynamic model is the complex expression of the model. The drawback of the power model is the loss of information due to the mix of torques. Indeed, the dynamic effect of the wrist is negligible compared to the effect of the first three axes.

The IV method is not affected by these problems because we keep all dynamic equations. In addition, the IV is less sensitive to the choice of cut-off frequency compared with the LS technique. From our point of view, our algorithm acts implicitly as an adaptive filter. Indeed, the high frequency noises are eliminated thanks to the integration of the MDD while the frequency bandwidth of our interest is determined by the bandwidth of the closed loop. Finally, experimental results have proven that the prefiltering is not necessary.

Another major improvement of our approach is to ensure the bandwidth of the closed loop in the simulator scheme. By this way, we have always $q_s, \dot{q}_s, \ddot{q}_s$ close to q, \dot{q}, \ddot{q} . The correlation between the instrument matrix and the observation matrix is still high because V is still close to W_{inf} . That means we ensure the crucial assumptions $E(V^T \rho) = 0$ and $V^T W$ invertible, and this explains why our algorithm works very well.

Our approach can be seen as an extension of the so-called SRIVC algorithm (Simplified Refined Instrumental Variable Continuous-time) adapted recently for closed loop system (Gilson et al. 2006) (Young, Garnier, et Gilson 2009). However, these algorithms are quite complicated and need prefiltering. They do not adapt the gain of the simulated feedback as it is proposed in this paper. Therefore, our method is not only an application of the IV to robotics but enrich the IV methodology by providing insights from robotics.

With our algorithm, the inverse and direct dynamic models are both validated at the same time. Up to now, the DDM was validated a posteriori in simulation. This is interesting for industrial applications because this algorithm saves time. In addition, if something goes wrong, that means the dynamic model is not valid since the IV method is robust to data filtering.

This paper has presented an extension and an application of the IV method. This technique was successfully applied on a 2 DOF prototype robot. From these experiments, it comes that our IV algorithm is not sensitive to data filter-

ing, gives additional improvements and can be helpful for practice. In addition, the convergence of the purposed algorithm is granted. Indeed, the bandwidth of the closed loop implemented to control the robot is ensured in the simulation. This is done by adapting the gains. Finally, it is also robust to the initialization.

However, to apply our algorithm properly, the structure of the control law applied to control the robot must be known.

Future works concern the use of this technique to identify flexibilities.

References

- Atkeson, C.G., C.H. An, et J.M. Hollerbach. 1986. Estimation of Inertial Parameters of Manipulator Loads and Links. *Int. J. of Robotics Research* 5, n° 3: 101-119.
- Davidson, Russell, et James Mackinnon. 1993. *Estimation and Inference in Econometrics*. Oxford University Press Inc, Juillet.
- Featherstone, R., et D.E. Orin. 2008. Dynamics. Dans *Springer Handbook of Robotics*. Vol. 2. Springer.
- Garnier, H., M. Gilson, et P.C. Cervellin. 2006. Latest developments for the matlab conssid toolbox. Dans *14th IFAC Symposium on System Identification, SYSID-2006*. Newcastle, Australia, Mars 29.
- Gautier, M. 1986. Identification of Robot Dynamics. Dans *Proc. of IFAC Symposium on Theory of Robots*, 351-356. Vienne, Austria, Décembre.
- . 1991. Numerical calculation of the base inertial parameters. *Journal of Robotics Systems* 8, n° 4: 485-506.
- . 1997. Dynamic Identification of Robots with Power Model. Dans *Proc. of IEEE International Conference on Robotics and Automation*, 1922-1927. Albuquerque, USA, Avril.
- Gautier, M., et W. Khalil. 1990. Direct calculation of minimum set of inertial parameters of serial robots. *IEEE Transactions on Robotics and Automation* 6, n° 6 (Juin): 368-372.
- . 1992. Exciting trajectories for the identification of the inertial parameters of robots. *International Journal of Robotics Research* 11, n° 4 (Août): 362-375.
- Gautier, M., et P. Poignet. 2001. Extended Kalman Filtering and Weighted Least Squares Dynamic Identification of Robot. *Control Engineering Practice* 9: 1361-1372.
- Gautier, M., P.O. Vandanjon, et C. Presse. 1994. Identification of inertial and drive gain parameters of robots. Dans *Decision and Control, 1994., Proceedings of the 33rd IEEE Conference on*, 4:3764-3769 vol.4. doi:10.1109/CDC.1994.411744. 10.1109/CDC.1994.411744.
- Gilson, M., H. Garnier, P.C. Young, et P. Van den Hof. 2006. A refined IV method of closed-loop system identification. Dans *14th IFAC Symposium on System Identification, SYSID-2006*, 903-908. Newcastle, Australia, Mars 29.
- Janot, A., C. Bidard, F. Gosselin, M. Gautier, D. Keller, et Y. Perrot. 2007. Modeling and Identification of a 3 DOF Haptic Interface. Dans *Robotics and Automation, 2007 IEEE International Conference on*, 4949-4955. doi:10.1109/ROBOT.2007.364242. 10.1109/ROBOT.2007.364242.
- Janot, A., P-O. Vandanjon, et M. Gautier. 2009. Identification of robots dynamics with the Instrumental Variable method. Dans *Proc. of IEE Int. Conf. on Robotics and Automation (ICRA)*, 1762-1767. Kobe, Mai.
- Khalil, W., et E. Dombre. 2002. *Modeling identification and control of robots*. Taylor and Francis, Mars.
- Khalil, W., M. Gautier, et P. Lemoine. 2007. Identification of the payload inertial parameters of industrial manipulators. Dans *Robotics and Automation, 2007 IEEE International Conference on*, 4943-4948. doi:10.1109/ROBOT.2007.364241. 10.1109/ROBOT.2007.364241.
- Khalil, W., et J.F. Kleinfinger. 1986. A new geometric notation for open and closed loop robots. Dans *Proc. of IEEE International Conference On Robotics And Automation*, 1147-1180. San Francisco, CA, USA, Avril.
- Khosla, P.K, et T. Kanade. 1985. Parameter Identification of Robot Dynamics. Dans *Proc. of 24th IEEE Conference on Decision and Control*, 1754-1760. Fort-Lauderdale, USA, Décembre 11.
- Kozłowski, Krzysztof. 1998. *Modelling and identification in robotics*. Springer.
- Lemaire, C-E, P-O Vandanjon, M. Gautier, et C Lemaire. 2006. Dynamic identification of a vibratory asphalt compactor for contact efforts estimation. Dans *14th IFAC Symposium on System Identification, SYSID-2006*. Newcastle, Australia, Mars 29.
- Middleton, R.H., et G.C. Goodwin. 1988. Adaptive computed torque control control for rigid link manipulator. *Systems and Control Letters* 10, n° 1: 9-16.
- Puthenpura, Sarat C., et Naresh K. Sinha. 1986. Identifica-

tion of Continuous-Time Systems Using Instrumental Variables with Application to an Industrial Robot. *Industrial Electronics, IEEE Transactions on IE-33*, n°. 3: 224-229. doi:10.1109/TIE.1986.350226.

- Raucent, B., G. Bastin, G. Campion, J-C. Samin, et P.Y. Willems. 1992. Identification of Barycentric Parameters of Robotic Manipulators from External Measurements. *Automatica* 28, n°. 5: 1011-1016.
- Restrepo, P.P., et M. Gautier. 1995. Calibration of drive chain of robot joints. Dans *Proc. of 4th IEEE Conf. on Control Applications*, 526-531. Albany, NY, USA, Septembre.
- Slotine, J.-J., et Weiping Li. 1987. Adaptive manipulator control a case study. Dans *Robotics and Automation. Proceedings. 1987 IEEE International Conference on*, 4:1392-1400.
- Söderström, Torsten, et Petre Stoica. 1989. *System identification*. Prentice Hall.
- Swevers, J., C. Ganseman, D-B. Tukel, J. DeSchutter, et H. VanBrussel. 1997. Optimal Robot Excitation and Identification. *IEEE Trans. on Robotics and Automation* 13, n°. 5 (Octobre): 730-740.
- Vandanjon, P-O., A. Janot, M. Gautier, et F. Khatounian. 2007. Comparison of two identification techniques: Theory and application. Dans *Proc. of the 4th International Conference on Informatics in Control, Automation and Robotics; SS on Fractional Order Systems (ICINCO)*, 341-347. Angers, Mai.
- Venture, G., P-J Riper, W Khalil, M. Gautier, et P. Bods-on. 2006. Modeling and identification of passenger car dynamics using robotics formalism. *IEEE Transactions on Intelligent Transportation Systems* 7, n°. 3 (Septembre): 349-355.
- Young, P.C. 2006. An instrumental variable approach to ARMA model identification and estimation. Dans *Proc. of 14th IFAC Symposium on System Identification, SYSID 2006*, 410-415. Newcastle, Australia, Mars 29.
- Young, P.C., H. Garnier, et M. Gilson. 2009. Simple Refined IV Methods of Closed-Loop System Identification. Dans *Proc. of 15th IFAC Symposium on System Identification, SYSID 2009*, 1151-1156. Saint-Malo (France), Juillet 6.
- Young, P.C., et A.J. Jakeman. 1979. Refined instrumental variable methods of time-series analysis: Part 1, SISO systems. *International Journal of Control* 29: 1-30.